JOURNAL: Ecological Applications 26(2) - March 2016

Queue No. 5520

ESA MS#: 14-1874

MANUSCRIPT TYPE: Article

TITLE: Space-time investigation of the effects of fishing on fish populations

AUTHORS: Kotaro Ono, Andrew Shelton, Eric Ward, James Thorson, Blake Feist, and Ray Hilborn

CORRESPONDING AUTHOR NAME: Dr. Kotaro Ono

CORRESPONDING AUTHOR EMAIL(S): kotarono@uw.edu

RUNNING HEAD: Not yet provided by author; please request as query at proof stage

RECEIVED DATE: 3 October 2014

REVISED DATE: 23 July 2015

ACCEPTED DATE: 24 July 2015

FINAL VERSION RECEIVED DATE (if >21 days after accepted date):

CORRESPONDING EDITOR: E. E. Plaganyi

SPECIAL NOTES: Eligible for Accepted Articles and Early View (ESA Preprint posted)

No. figures (total): 8

No. color figures: 3

No. tables: 2

This is the author manuscript accepted for publication and has undergone full peer review but has not been through the copyediting, typesetting, pagination and proofreading process, which may lead to differences between this version and the Version of Record. Please cite this article as doi: 10.1002/EAP.1229

This article is protected by copyright. All rights reserved

Author Manuscript

Total no. supporting information files: 3 individual files plus 1 ZIP file

Total no. files: 5

File names: 14-1874_Ono_Manuscript.docx

14-1874_Ono_AppendixA.docx

14-1874_Ono_AppendixB.docx

14-1874_Ono_AppendixC.docx

14-1874_Ono_Supplement_Rcodes.zip

12/21/15 - HC

Author Manuscript

This article is protected by copyright. All rights reserved

Received Date: 03-Oct-2014
Revised Date: 23-Jul-2015
Accepted Date: 24-Jul-2015
Article Type: Original Article
MS14-1874 Ono
Article

Space-time investigation of the effects of fishing on fish populations

Kotaro Ono,[1,4] Andrew O. Shelton,[2] Eric J. Ward,[2] James T. Thorson,[3] Blake E. Feist,[2] and Ray Hilborn[1]

[1]School of Aquatic and Fishery Sciences, Box 355020, University of Washington, Seattle, Washington 98195-5020 USA

[2]Conservation Biology Division, Northwest Fisheries Science Center, National Marine Fisheries Service, National Oceanographic and Atmospheric Administration, 2725 Montlake Blvd E, Seattle, Washington 98112 USA

[3]Fisheries Resource Analysis and Monitoring Division, Northwest Fisheries Science Center, National Marine Fisheries Service, National Oceanographic and Atmospheric Administration, 2725 Montlake Blvd E, Seattle, Washington 98112 USA

Manuscript received 3 October 2014; revised 23 July 2015, accepted 24 July 2015.
Corresponding Editor: E. e. Plaganyi.

[4] E-mail: kotarono@uw.edu

Abstract.

Species distribution models (SDMs) are important statistical tools for obtaining ecological insight into species–habitat relationships and providing advice for natural resource management. Many SDMs have been developed over the past decades, with a focus on space- and more recently, time-dependence. However, most of these studies have been on terrestrial species and applications to marine species have been limited. In this study, we used three large spatio-temporal data sources (habitat maps, survey-based fish density estimates, and fishery catch data) and a novel space-time model to study how the distribution of fishing may affect the seasonal dynamics of a commercially important fish species (Pacific Dover sole, Microstomus pacificus) off the west coast of the USA. Dover sole showed a large scale change in seasonal and annual

This article is protected by copyright. All rights reserved

Author Manuscript

distribution of biomass, and its distribution shifted from mid-depth zones to inshore or deeper waters during late summer/early fall. In many cases, the scale of fishery removal was small compared to these broader changes in biomass, suggesting that seasonal dynamics were primarily driven by movement and not by fishing. The increasing availability of appropriate data and space-time modeling software should facilitate extending this work to many other species, particularly those in marine ecosystems, and help tease apart the role of growth, natural mortality, recruitment, movement, and fishing on spatial patterns of species distribution in marine systems.

Key words: fishing; habitat; marine species; Microstomus pacificus; movement; Pacific Dover sole; space-time model; species distribution.

INTRODUCTION

A central aim in conservation is to preserve important habitats for organisms to ensure species and population persistence in the face of anthropogenic threats (ESA 1973, Kareiva et al. 2008). Species distribution models have proven vital as tools for expanding our understanding of species habitat associations and for conservation planning and resource management (Guisan and Thuiller 2005, Elith and Leathwick 2009). Many methods have been developed over the past several decades to model the distribution of species in relation to habitat. Statistical techniques include generalized linear models (GLMs), generalized additive models (GAMs), quantile regression, artificial neural networks, regression trees, and genetic algorithms (see reviews by Guisan and Thuiller 2005, Elith and Leathwick 2009). To date, however, many of these models have failed to consider space and time dependence (Dormann 2007, Hoeting 2009). Explicitly accounting for space-time dependence is crucial for understanding current and future threats from anthropogenic forces and for reducing the risks of erroneous results as many exogenous (e.g., climate, habitat) and endogenous (e.g., dispersal, predation) drivers of species distributions are likely to vary through time and space (Legendre 1993, Hoeting 2009, Cressie and Wikle 2011).

Despite the importance of spatial and temporal processes in biology, the use of space-time models has remained limited due to their presumed complexity and computational burden. The number of numerical operations increases quickly as the dimensionality of models in space and time increases, rendering computation slow and sometimes infeasible for large datasets. Nonetheless, space-time modeling has become more feasible and accessible through the availability of several statistical software packages in the last decade, owing to the increasing

This article is protected by copyright. All rights reserved

Author Manuscript

computational power and advances in numerical techniques (e.g., R, WinBUGS, Matlab, SAS). Furthermore, sophisticated methods have been developed to deal with spatio/temporal dependence including sparse matrix operations (e.g., covariance tapering; Furrer et al. 2006), predictive process models (Banerjee et al. 2008, Latimer et al. 2009, Finley et al. 2009), numerical approximation to the likelihood (e.g., spectral methods; Fuentes 2007), or the use of Markov random fields (Rue and Martino 2007). Several biological, environmental, and natural resource studies have used these techniques to model the distribution of disease (Schrödle and Held 2011), weather (Finley et al. 2012), heritability (Holand et al. 2013), animals and plants (Latimer et al. 2009, Thorson et al. 2015, Ward et al. 2015), at a variety of geographical and temporal scales.

In marine ecosystems, many factors could potentially affect the distribution of fish over time and space (Whittaker et al. 1973). Fish may have a specific habitat preference that can vary with life stage. The mobility of a species can also vary with ontogeny and scale (sedentary vs. mobile species; diurnal, ontogenetic, or seasonal movement), and they interact with their prey and predators. Humans are one of the central predators in marine ecosystems and can alter fish communities substantially (Worm et al. 2009). Moreover, fishing does not occur randomly in space and time as fishers choose the location and timing of fishing based on their knowledge and the rules that regulate fisheries (Holland and Sutinen 2000, Branch et al. 2006, van Putten et al. 2012). As a consequence, marine species distributions can potentially change over relatively short periods of time, with the change in distribution reflecting the joint effect of fishing activity, environment, and species life history.

In this study, we introduce a modelling framework that allows us to tease apart the effect of fishing from other factors, such as movement, recruitment, natural mortality, or growth, based on the analysis of how species and fishery catches are distributed in space and time. To do so, we make use of the three large-scale spatio-temporal data sources and the unique design of the research survey (parallel surveys conducted three months apart in the summer and fall) to examine how population changed between these two time periods and whether changes were related to fishing activities. The three spatio-temporal data sources are detailed benthic habitat data from the continental shelf and slope off the west coast of the USA, fish density estimates from an extensive fishery-independent research survey, and commercial fishing catch data. We focus our analysis on the dynamics of Pacific Dover sole (Microstomus pacificus), an abundant

This article is protected by copyright. All rights reserved

Author Manuscript

and commercially important species as a case study, to illustrate the applicability of our methodology to study the seasonal dynamics of any marine species. Our approach is broad and may be applied to virtually any species targeted by commercial or recreational hunters or fishers where appropriate data are available.

MATERIAL AND METHODS

Motivational case study: Dover sole population of the U.S. west coast

Dover sole is a commercially important flatfish species off the U.S. west coast (Fig. 1) that has been exploited since the early 20th century (Hicks and Wetzel 2011). The annual catch over the last fifty years averages 14000 tons (~2% exploitation rate), and in 2012, the landed value of the catch was estimated at over US$6.5 million. The species is long-lived (maximum age ~60 yr) and widely distributed from Alaska to southern California. It is commonly found on sandy/muddy ocean bottoms, in waters ranging from 37 to 1500 m. Individual Dover sole tend to migrate to deeper waters in winter (between November and March), during the spawning season (Hagerman 1952) and as they mature and age (Jacobson et al 2001).

NOAA's Northwest Fisheries Science Center (NWFSC) conducts fishery-independent surveys using bottom trawl gear to assess the spatio-temporal distribution of Dover sole and other co-occurring species (Bradburn et al. 2011). In this study, we use data from 2004 to 2011. The survey involves two passes each year: the first pass occurs between mid-May and August, while the second pass lasts from August to October. Approximately 700 hauls are conducted each year. A standard trawl net is towed through the water for 15 min, and the number and biomass of all fish present are recorded along with the spatial location, average depth, and bottom temperature. We used the midpoint between the start and end of each haul as the location of the catches. We complemented this data using additional habitat information, i.e., sediment grain size and distance to nearest rock outcrops derived from NMFS (2013). Detailed descriptions of the sampling design, gear, and protocols used for this survey are found in Keller et al. (2012).

In addition to the spatially referenced survey data, we also used nearly 200000 spatially referenced commercial Dover sole catch records by fishing vessels. It is mandatory for fishers to report all trawl events, however, logbook data are often incomplete, with only 90% of the reported Dover sole catch recorded. We therefore assumed that the missing catches in the logbook data were missing-at-random, and they were imputed randomly based on multinomial distribution with the expected catch probabilities obtained from the logbook data on a 2 × 2 km

This article is protected by copyright. All rights reserved

Author Manuscript

grid. This created a map of catch distribution for each grid and each area. Catch data at the tow level were evenly distributed to each grid based on the portion of commercial vessel tracks intersecting each of the 2 × 2 km grids.

General approach

The first objective of this study is to examine how Dover sole distribution changed from summer to fall, or fall to summer in each year between 2004 and 2011. A second objective is to identify potential causal mechanisms for any changes (fishing or other biological mechanisms, such as ontogenetic movement, natural mortality, recruitment, and growth). In other words, we ask whether the fall research vessel survey (or late spring survey) shows any changes in biomass compared to the late spring survey (or fall survey) and if any such changes can be attributed to fishery removals and/or to other factors such as growth, movement, natural mortality, and recruitment.

Our statistical approach involves several steps, summarized briefly here. First, we fit a statistical model to the survey data to determine the spatial distribution of Dover sole by year and survey pass. Second, we used those space-time models to predict the biomass of Dover sole along the coast for each pass and year. Third, we calculated the net change in biomass between the survey passes after taking the catch into account. Finally, we examined any residual patterns of variation in the net change in biomass and determined if the pattern could be explained by any environmental and/or biological factors.

Estimating population biomass at each survey pass

Description of the space-time regression model.— We fitted a space-time generalized linear model (GLM) to the survey data (n_{obs} = 5193) to create a predictive map of population biomass along the U.S. west coast for each survey pass and year. We modeled the species distribution in two stages: first, a space-time model was fit to explain the variation in Dover sole presence/absence; then a second model for the positive data was fit to explain changes in Dover sole density given that a least one fish was observed (see also Shelton et al. 2104 and Ward et al. 2015). We used this modeling framework because survey data comprised a large portion of zeros (17% of the data) and we expected different variables to be important to for the presence/absence and positive stages of the model. These two pieces were assumed to be conditionally independent, and the general framework is often referred as a delta or hurdle model in ecology (Zuur et al. 2009). We constructed our model in a Bayesian framework (see Table 1 for prior

This article is protected by copyright. All rights reserved

Author Manuscript

specification). Separate models were created for each survey pass as the objective of the study was to determine changes in population distribution between the two survey passes each year. Occurrence of Dover sole at a set of locations **S**, year t and survey pass p, $\boldsymbol{\pi_{p,t}(S)}$ was modeled using a binomial GLM with logit link

$$\text{logit}\left(\boldsymbol{\pi_{p,t}(S)}\right) = \boldsymbol{X_{p,t}(S)b_p} + \boldsymbol{\omega_{p,t}(S)}$$

where $\mathbf{X_{p,t}(S)}$ is a matrix of covariates at locations **S**, year t, and pass p, $\mathbf{b_p}$ is the vector of regression coefficients (shared across years for each pass p for continuous variables; we assumed that fish preference for these habitat variables does not change between years for each pass p during this short study period), and $\mathbf{w_{p,t}}$ is the spatial field for year t and pass p. The covariates used in this study are log(depth), $(\log(\text{depth}))^2$, temperature, temperature^2, sediment size, sediment size^2, distance to rock, and fixed year effect (more details on the choice of covariates are given later and in Appendix A). We also assumed that the spatial field is independent and different between years. In this sense, our model is not a typical spatio-temporal model as implied by the spatio-temporal statistical literature (e.g., Cressie and Wikle 2011).

To model the non-zero Dover sole density (kg/km^2; over all size and age classes) at a set of locations **S**, year t, and survey pass p, $\boldsymbol{\mu_{p.t}(S)}$, we assumed that the log of Dover sole density was normally distributed.

$$\log\left(\boldsymbol{\mu_{p.t}(S)}\right) = \boldsymbol{Z_{p,t}(S)a_p} + \log\left(\boldsymbol{E_p(S)}\right) + \boldsymbol{\delta_{p,t}(S)}$$

where $\mathbf{Z_{p,t}(S)}$ is a matrix of covariates at locations **S**, year t, and pass p, (similar to $\mathbf{X_{p,t}(S)}$), $\mathbf{a_p}$ is the vector of regression coefficients, $\boldsymbol{\delta_{p,t}}$ is the spatial field for year t and pass p (we assumed again that the spatial field is independent between years), and $\mathbf{E_p(S)}$ represents the swept areas of the tows (and modeled as an offset variable).

The estimation of spatial field involves choosing (1) the correlation structure between neighboring cells and (2) how the spatial field changed over time. In this study, we modeled the spatial field $\mathbf{w_{p,t}}$ (and $\boldsymbol{\delta_{p,t}}$) as a smooth spatial surface, $\mathbf{w_{p,t}} \sim \text{MVN}(0, \boldsymbol{\Sigma_{p,t}} = \tau_p^2 \mathbf{C_{p,t}}(h))$ where τ_p^2 is the spatial variance and $C_{p,t}(h)$ is the isotropic spatial correlation function defined by the Matérn function with $\nu = 0.5$ (Lindgren et al. 2011; similar to the exponential function in this case). We assumed that the spatial field was independent between years. In this way, we account for the possibility for inter-annual changes in species distribution with a distinct clustering pattern for each year (as in Shelton et al. 2014).

This article is protected by copyright. All rights reserved

Author Manuscript

$$\Sigma_p = \begin{bmatrix} \Sigma_{p,2004} & 0 & \dots & 0 \\ 0 & \Sigma_{p,2005} & & \vdots \\ \vdots & & \ddots & 0 \\ 0 & \dots & 0 & \Sigma_{p,2011} \end{bmatrix}$$

Model fitting was performed using the R package INLA (Blangiardo et al. 2013) and readers are referred to Rue et al. (2009), Lindgren et al. (2011), and Cameletti et al. (2013) for details about the underlying theory and computational approaches for space-time models using INLA (see the Supplement for R codes).

Explanatory variables.—We used existing geospatial data layers from the Essential Fish Habitat (EFH) Phase 1 report (NMFS 2013), which included depth, sediment grain size, bottom temperature, and distance to nearest rocky habitat (at least 1 ha in area; see Appendix A for details on habitat covariates). These variables are important habitat characteristics that can potentially affect the distribution of marine fish (Allen et al. 2006). Distance to rock was calculated using ArcGIS software to calculate the distance from each of the trawl survey sites to the nearest rock habitat patch (see NMFS 2013). We only used rocky patches greater than 1 ha in area.

Model selection.—Model selection was conducted to decide which of the explanatory variables to include in the models. The explanatory variables available for this study were log(depth), $(\log(\text{depth}))^2$, distance to nearest rocky habitat, sediment grain size, $(\text{sediment grain size})^2$, temperature, and $(\text{temperature})^2$. Model selection was based on the deviance information criteria (DIC; Spiegelhalter et al. 2002) and the mean logarithmic score (Gneiting and Raftery 2007, Krnjajić et al. 2008); two metrics that are readily available from the INLA model output. In either case, the lower the metric, the more preferred the model. The DIC was directly obtained from the model output while the logarithmic score (LS) was calculated as the negative log of the conditional predictive ordinate (CPO). The CPO corresponds to the position of the observed value y_i within the leave-one-out cross-validatory posterior predictive distribution evaluated at the observed value y_i. A paired permutation test based on the observation-level score provided a convenient approach to test if one model's mean logarithmic score was significantly different than another one.

$$\overline{\text{LS}} = \frac{\sum_{i=1}^{n_{obs}} \left(-\log\left(\text{CPO}_i\right)\right)}{n_{obs}}$$

where n_{obs} corresponds to the number of data points (n_{obs}= 5193).

This article is protected by copyright. All rights reserved

Author Manuscript

Moving up from density to estimate of population biomass along the coast.—We computed the posterior predictive distribution for Dover sole density at each pass and year once the best models for each pass was chosen (one for the presence/absence and one for the positive catch data; see Appendix A for details about the projection grid). We generated the unconditional posterior predictive distribution for fish density, $I_p(\mathbf{S},t)$, for each 2 × 2 km grid along the coast (i.e., beyond the sampled locations, for a total of 38047 grid cells) by calculating the product of the two models' prediction: the probability of fish presence at each grid and the probability distribution of fish density assuming that fish were present. The distribution reflected the biomass susceptible to the trawl gear, not the entire population, because the bottom trawl does not catch fish of different sizes equally (i.e., selectivity varied with length), and fish population size structure was unknown. We therefore needed to re-scale the whole distribution to match the scale of the exploitable population size (age 5+) estimated in the latest Dover sole assessment (Hicks and Wetzel 2011). To do so, the scaling coefficients q_1 and q_2 (also called catchability coefficient in the fisheries literature; Maunder and Punt 2004) were calculated as the average ratio (between 2004 and 2011) between the total mean predicted population density from passes 1 and 2 in year t, $\bar{I}_p(\mathbf{S},t)$, and the exploitable population size in year t estimated in the actual assessment, $\text{Biomass}_t^{\text{assesssment}}$.

$$q_1 = \frac{1}{8}\sum_{t=2004}^{2011}\left(\frac{\sum_{S=1}^{N}\bar{I}_{p=1}(\mathbf{S},t)}{\text{Biomass}_t^{\text{assessment}}}\right) = 0.25$$

$$q_2 = \frac{1}{8}\sum_{t=2004}^{2011}\left(\frac{\sum_{S=1}^{N}\bar{I}_{p=2}(\mathbf{S},t)}{\text{Biomass}_t^{\text{assessment}}}\right) = 0.24$$

Finally, Dover sole biomass at location **S**, $B_p(\mathbf{S},t)$, for each pass p and year t, was determined by dividing the density index by the scaling coefficients.

$$B_{p=1}(\mathbf{S},t) = \frac{I_{p=1}(\mathbf{S},t)}{q_1}$$

$$B_{p=2}(\mathbf{S},t) = \frac{I_{p=2}(\mathbf{S},t)}{q_2}$$

This article is protected by copyright. All rights reserved

Author Manuscript

Calculating the net change in biomass (NCB) between the two survey passes

There is a gap of roughly two and a half months between the starting dates of the two survey passes within a year. During that time, biomass at a given location can change due to fishing, growth, natural mortality, recruitment, and movement. By calculating the change in biomass between the two passes after taking into account the fishery removals, we can measure the cumulative effect of growth, natural mortality, recruitment, and movement over time and space. We refer to this quantity as the net change in biomass (NCB). NCB can be calculated for two time periods: (1) between pass 1 and pass 2 of the same year, $NCB_1(\mathbf{S},t)$, or (2) between pass 2 of year t and pass 1 of year t+1, $NCB_2(\mathbf{S},t)$. In other words, $NCB_1(\mathbf{S},t)$ measures the change from summer to fall of the same year, and $NCB_2(\mathbf{S},t)$ measures the change from fall to summer of the next year.

$$NCB_1(S,t) = B_{p=2}(S,t) - B_{p=1}(S,t) + Catch_1(S,t)$$
$$NCB_2(S,t) = B_{p=1}(S,t+1) - B_{p=2}(S,t) + Catch_2(S,t)$$

where $Catch_1$ and $Catch_2$ are the total fishery removals from grids **S** between pass 1 and 2 of the same year or pass 2 of year t and pass 1 of year t + 1, respectively. In practice, the distributions of NCB_1 and NCB_2 are determined based on MCMC samples (1000) from the biomass distributions at pass 1 and 2, and a Monte Carlo sample (1000) from the catch distribution (as these parameters were calculated independently in this study). This Monte Carlo approach appropriately propagates uncertainty in both the biomass and catch throughout the analyses. There are at least three possible hypotheses for our analyses of net change in biomass. If both NCB_1 and NCB_2 are close to zero, this suggests that fishery removals are the main factor explaining the changes in biomass between the two passes and there is not a substantive contribution of growth or movement. If NCB_1 and NCB_2 differ from zero and show opposite patterns when plotted against a covariate, we can speculate that seasonal movement is the main factor affecting the changes in biomass (e.g., fish moving nearshore to feed then moving to deeper waters to reproduce). If growth, natural mortality, or recruitment is the main factor driving the spatial patterns, we would expect NCB_1 and NCB_2 be different from zero but NCB_2 would not mirror the changes NCB_1 as fall patterns of growth, natural mortality, and recruitment are not expected to be related to the summer pattern.

Detecting pattern of variation in the net change in biomass along the coast

This article is protected by copyright. All rights reserved

Author Manuscript

In order to analyze the pattern of variation in net change in biomass along the coast, we need to extract the marginal effect of each covariate on NCB_1 and NCB_2. This is not straightforward for several reasons. First, the net change in biomass is affected by fishery removal which reflects fishermen behavior. NCB_1 and NCB_2 are therefore affected by complex interaction between variables (fishermen might choose to fish in specific depth range at a specific time). A second difficulty is that the net change in biomass in each grid and time is not known but rather has a distribution that reflects its uncertainty. To deal with these issues, we couple the use of a random forest algorithm (RF; see Breiman 2001 or Cutler et al. 2007 for detailed explanation of RF), to extract the marginal effect of different variables on the net change in biomass, with the Monte Carlo (MC) sampling methodology, to account for uncertainty in net change in biomass. RF is a powerful machine learning algorithm that can handle complex interaction between variables and provides user friendly graphical visualization of the marginal effect of independent variables to the dependent variable through partial dependence plots. In short, RF works as follow: (1) create many bootstrap data (n_{tree}) from the original data; (2) fit a regression tree (in this study) to each bootstrap data by only using a random subset of predictors at each node (m_{try}); (3) predict new data by averaging the prediction from all n_{tree} regression trees. We implemented RF using the package "randomForest" in R (Liaw and Wiener 2002). To account for the distribution uncertainty in NCB_1 and NCB_2, we ran the RF analysis 100 times (the results did not qualitatively change after 50) with different Monte Carlo samples of NCB_1 and NCB_2 for each year. For each RF analysis, we included depth, Northing (i.e., northward-measure of distance, similar to latitude), distance to closest rock outcrops, sediment size, and a random variable varying from [0, 1] as explanatory variables to examine if/how the latter affected the changes in net change in biomass. We incorporated the random variable to examine the importance of the other covariates. Again, if the marginal effect plots show an opposite pattern between NCB_1 and NCB_2, movement is suggested as the main reason behind these seasonal changes in biomass. If catch is the main factor affecting the changes in biomass between the two passes, we would expect the net change in biomass be close to zero.

RESULTS

The best models (Table 2) fit the data well and explained a higher portion of variability in catch rates than conventional design-based estimator as seen in Thorson et al. (2015; see Appendix B for the posterior distributions of model parameters).

This article is protected by copyright. All rights reserved

Author Manuscript

How does Dover sole biomass change between survey passes and among years?

Our analyses showed clusters of high biomass along the coast and high variability in Dover sole distribution among years and survey passes (Fig. 2). Dover sole was generally abundant in the 200–800 m depth zone (Fig. 3) but seemed to have shifted toward deeper area between pass 1 and 2 (Fig. 3). A cluster of high Dover sole biomass was present for few years northwest and southwest of San Francisco (especially for pass 1) and between Cape Blanco and Astoria (Fig. 2).

Does biomass change in response to fishing?

In general, we found little evidence for fishing impacts on changes in biomass (Fig. 4). While most of the catches were recorded below 5 tons in each grid (totaled across grids catches averaged 8500 tons annually over the last eight years), the scale of biomass change between the survey passes was much higher, and varied frequently from −200 to 200 tons (Fig. 4).

How does the net change in biomass vary spatially and temporally? Are there consistent patterns of net change in biomass among years?

We detected spatial areas where population biomass changed dramatically between seasons with both areas of large positive or negative NCB (Fig. 5; dark green and dark red areas, respectively). However, the magnitude and location of these areas with large NCB varied across years. For example, areas with negative NCB_1 (red color; indicative of reduced Dover sole biomass in the fall relative to the summer) were concentrated between San Francisco and Eureka in 2006 and 2007, but move northward in 2009 to between Eureka and Astoria (Fig. 5). Similarly, the distribution of NCB_2 varied among years, with a pattern that was generally opposite of NCB_1. Despite the year to year variation in NCB_1 and NCB_2, some areas along the coast showed consistent negative or positive net change in biomass between the survey passes (Figs. 5 and 6b, c). For example, one region northwest of Eureka, one northwest of San Francisco, and one southwest of San Francisco showed a consistently negative NCB_1 (across year median; Fig. 6b, c). In contrast, median NCB_1 was positive southwest of Cape Flattery, west of Astoria, and northwest of Point Conception. NCB_2 showed a strong negative correlation with NCB_1 (Fig. 6d), with positive areas northwest of Eureka, northwest and southwest of San Francisco, negative southwest of Cape Flattery, and west of Astoria.

How does the net change in biomass change with respect to environmental covariates?

Northing (latitude) affected NCB_1 and NCB_2 in a complex manner (Figs. 7d and 8d). Northmost (above 1500 km north, i.e., along the Washington coast) and southmost regions (below 200 km

This article is protected by copyright. All rights reserved

Author Manuscript

north, i.e., south of Point Conception) had a higher average NCB_1 across years than the rest of the coast (Fig. 7d). 2004 and 2005 was notable with an overall net change in biomass much higher than the rest of the years. Similarly, average NCB_1 dropped below zero around 700 km and 1100 km north with some year to year variability. All these locations corresponded to the regions previously identified with consistent positive or negative NCB_1 across years (Fig. 6b). The average NCB_2 showed almost exactly the opposite pattern than the average NCB_1 with negative estimates in northmost and southmost areas for example (Fig. 8d).

Similarly to the effect of Northing on NCB_1, there was a large year to year fluctuation in the effect of depth to the NCB_1 (Fig. 7e). On average, shallow (<100 m) and deeper (>700 m) areas had a higher NCB_1 estimates than intermediate-depth areas (100, 700 m). However, the depth range with positive or negative NCB_1 varied depending on the year. As an example, NCB_1 was positive from (0–700 m) in 2004 while it was negative in 2007. Here again, the pattern in NCB_2 was almost the opposite of that of NCB_1 (Fig. 8e).

Finally, NCB_1 was on average decreasing for increasing distance to rock (Fig. 7f) and sediment size did not affect strongly the value of NCB_1 (Fig. 7g). But again, NCB_2 varied in the opposite manner compared to NCB_1 (Fig. 8f, g).

DISCUSSION

Pattern in Dover sole biomass change along the U.S. west coast: potential causes and consequences

Despite its economic importance, exploitation rates for Dover sole have been quite low in recent years (Hicks and Wetzel 2011). As a consequence, most of the observed changes in biomass in space and time for Dover sole were likely due to factors other than fishing. Our results are consistent with movement as the primary driver of Dover sole seasonal dynamics: NCB_1 values were negatively correlated with NCB_2 values across years and space (Fig. 6) and RF partial dependence plots showed that net change in biomass was changing in the opposite direction with respect to environmental covariates between NCB_1 and NCB_2 (Figs. 7 and 8). We detected three factors potentially influencing the movement of Dover sole: depth, latitude, and the presence of rock outcrops.

Between summer and fall, Dover sole biomass decreased on average at intermediate depth (100, 700 m) to increase in shallow (<100 m) and deeper waters (>700 m; Fig. 7e). There are at least two possible explanations for these observations. First, Toole et al. (2011) noted that juvenile

This article is protected by copyright. All rights reserved

Author Manuscript

Dover sole (10–22 cm) tended to move inshore (depth <150 m) during summer. Summer coastal upwelling brings nutrient-rich water from the deep to the shallow waters off the west coast of the USA, increasing its primary productivity and creating favorable conditions for juvenile Dover sole (Landry et al. 1989). The positive change in biomass observed in shallow waters in late summer/early fall might therefore reflect movement of juvenile Dover sole into these nursery grounds. As for the flux of biomass in deeper water, this could be related to the ontogenetic movement of Dover sole as they grow and mature (Jacobson et al. 2001). While we hypothesized that seasonal movement might be responsible for these patterns in population change, we cannot exclude the possibility of differential growth, natural mortality, or recruitment. However, such massive and temporally consistent spatial variation in growth, natural mortality, or recruitment is an unlikely explanation as it would require temporally consistent and successive events of fish recruitment (or growth) followed by natural death (and vice versa) at the exact same location. Dover sole biomass also changed in a complex manner between summer and fall as a function of latitude (Figs. 7d and 8d). NCB_1 indicated that Dover sole congregated in the late summer along the Washington coast (>1500 km north) and south of Point Conception, and left regions such as northwest and southwest of San Francisco and northwest of Eureka (Fig. 6b). Although the origin of these fish could not be determined using the current methodology, a parsimonious explanation is that fish moved from nearby areas (as suggested by comparing NCB_1 and NCB_2). Finally, Dover sole net change in biomass was estimated to be decreasing with distance to rock during summer (Fig. 7f). This is a surprising result, given previous studies that have suggested that Dover sole generally prefer sandy/muddy bottom. However, some flatfish species such as Petrale sole could be found in high concentration in sandy bottom close to rocky habitats (A. Hicks, personal communication).

The importance of spatial and temporal dependency in species distribution modeling

Space-time models are increasingly important in ecology (Dormann et al. 2007, Beale et al. 2010, Saas and Gosselin 2014). However, many ecological studies still ignore spatial and/or temporal dependence (Dormann 2007). This is the case in marine systems where spatio-temporal data are commonly used to generate indices of total biomass but the spatial or space-time correlation structure of observations is generally ignored (Maunder and Punt 2004, Thorson and Ward 2013, Thorson et al. 2015). In this study, we have shown that space-time modeling is a versatile method that could easily be applied to answer practical problems such as (1) examining the

This article is protected by copyright. All rights reserved

Author Manuscript

change in the spatial distribution of a species within or between years, (2) looking at the impact of exploitation to the local population structure, (3) detecting patterns of population change and its relation to biological phenomena. As more georeferenced survey data become available to the public (e.g., http://oceanadapt.rutgers.edu/), we expect these approaches to be more widely used. Moreover, space-time models are important for the analysis of spatial data to reduce the risk of producing unreliable or inaccurate parameter estimates (Dormann 2007, Beale et al. 2010, Saas and Gosselin 2014). While data are becoming easier and cheaper to acquire, we rarely have data on all influential environmental variables. The inclusion of spatial (or temporal) autocorrelation in the model provides a flexible way to account for factors not explicitly included in the model (Dormann 2007, Beale et al. 2010, Saas and Gosselin 2014, Shelton et al. 2014).

CONCLUSION AND FUTURE WORK

The use of habitat variables in species distribution modeling and biomass estimation has a long history in terrestrial ecosystems, but basic habitat information has been lacking in marine ecosystems until the past decades or so. While these data have been used to inform the location of marine reserves (Ward and Vanderklift 1999, Sunblad et al. 2011) or for the identification of vulnerable and critical habitat (Krigsman et al. 2012), they have rarely been integrated into models of fish distribution (Robinson et al. 2011, Shelton et al. 2014, Ward et al. 2015). In this study, we took advantage of newly available spatio-temporal data on fish density and habitat and incorporated it into a space-time model to identify potential causal mechanisms (fishing or other biological mechanisms such as ontogenetic movement, recruitment, natural mortality, and growth) explaining the seasonal dynamics of Dover sole across the U.S. west coast. Dover sole dynamics appeared to be mainly described by seasonal movement along the coast and not by fishing. The species moved to shallow and deeper water between early summer and early fall following their ontogeny. They also appeared to move northmost and southmost in late summer and aggregate along the Washington coast and south of Point Conception, while leaving regions such as northwest and southwest of San Francisco and northwest of Eureka. Furthermore, our results seemed to be quite robust to the assumptions made in this study. A sensitivity test on the choice of q value (the catchability coefficient), and the choice of covariates (see Appendix C) showed that the main results did not change qualitatively; the same regions along the coast showed the consistent loss or gain in population and the three habitat covariates (depth, Northing, and distance to nearest rock outcrops) affected the net change in biomass in a similar pattern.

This article is protected by copyright. All rights reserved

Author Manuscript

In summary, spatially referenced catch and survey data indicated considerable year to year and season to season variability in the spatial distribution of Dover sole. These changes were mostly attributed to movement but growth, natural mortality, and recruitment could be factors that can also shape the population. Our methodology can be easily extended to other marine species to help tease apart the role of fishing, growth, natural mortality, recruitment, and movement on spatial patterns in production (i.e., NCB). This is all the more important as more data (e.g., http://oceanadapt.rutgers.edu/) and space-time modeling software become available to the general public. Among the list of species candidates, it would be interesting to expand the study to species with stronger fishing pressure to contrast with species such as Dover sole which has a low exploitation rate.

ACKNOWLEDGEMENTS

K. Ono was was partially funded by the Joint Institute for the Study of the Atmosphere and Ocean (JISAO) under NOAA Cooperative Agreement NA10OAR4320148, Contribution No. 2421. We thank Allan Hicks, André E Punt, Trevor A. Branch, Will Satterthwaite, two anonymous reviewers, and Éva Plagányi for their insightful comments on the manuscript.

LITERATURE CITED

Allen, L. G., D. J. Pondella, and M. H. Horn. 2006. Ecology of marine fishes: California and adjacent waters. University of California Press, Berkeley, California, USA.

Banerjee, S., A. E. Gelfand, A. O. Finley, and H. Sang. 2008. Gaussian predictive process models for large spatial data sets. Journal of the Royal Statistical Society Series 70:825–848.

Beale, C. M., J. J. Lennon, J. M. Yearsley, M. J. Brewer, and D. A. Elston. 2010. Regression analysis of spatial data. Ecology Letters 13:246–64.

Blangiardo, M., M. Cameletti, G. Baio, and H. Rue. 2013. Spatial and spatio-temporal models with R-INLA. Spatial and Spatio-temporal Epidemiology 7:39–55.

Bradburn, M. J., A. A. Keller, and B. H. Horness. 2011. The 2003 to 2008 U.S. West Coast bottom trawl surveys of groundfish resources off Washington, Oregon, and California: estimates of distribution, abundance, length, and age composition. U.S. Department of Commerce, National Oceanic and Atmospheric Administration, Northwest Fisheries Science Center, Seattle, Washington, USA.

Branch, T. A., et al. 2006. Fleet dynamics and fishermen behavior: lessons for fisheries managers. Canadian Journal of Fisheries and Aquatic Sciences 63:1647–1668.

This article is protected by copyright. All rights reserved

Author Manuscript

Breiman, L. 2001. Random forests. Machine Learning 45:5–32.

Cameletti, M., F. Lindgren, D. Simpson, and H. Rue. 2013. Spatio-temporal modeling of particulate matter concentration through the SPDE approach. AStA Advances in Statistical Analysis 97:109–131.

Cressie, N. A., and C. K. Wikle. 2011. Statistics for spatio-temporal data. Wiley, Hoboken, New Jersey, USA.

Cutler, D. R., T. C. Edwards, K. H. Beard, A. Cutler, K. T. Hess, J. Gibson, and J. J. Lawler. 2007. Random forests for classification in ecology. Ecology 88:2783–92.

Dormann, C. F. 2007. Effects of incorporating spatial autocorrelation into the analysis of species distribution data. Global Ecology and Biogeography 16:129–138.

Dormann, C. F., et al. 2007. Methods to account for spatial autocorrelation in the analysis of species distributional data: a review. Ecography 30:609–628.

Elith, J., and J. R. Leathwick. 2009. Species distribution models: ecological explanation and prediction across space and time. Annual Review of Ecology, Evolution, and Systematics 40:677–697.

Finley, A. O., S. Banerjee, and A. E. Gelfand. 2012. Bayesian dynamic modeling for large space-time datasets using Gaussian predictive processes. Journal of Geographical Systems 14:29–47.

Finley, A. O., H. Sang, S. Banerjee, and A. E. Gelfand. 2009. Improving the performance of predictive process modeling for large datasets. Computational Statistics and Data Analysis 53:2873–2884.

Fuentes, M. 2007. Approximate likelihood for large irregularly spaced spatial data. Journal of the American Statistical Association 102:321–331.

Furrer, R., M. G. Genton, and D. Nychka. 2006. Covariance tapering for interpolation of large spatial datasets. Journal of Computational and Graphical Statistics 15:502–523.

Gneiting, T., and A. E. Raftery. 2007. Strictly proper scoring rules, prediction, and estimation. Journal of the American Statistical Association 102:359–378.

Guisan, A., and W. Thuiller. 2005. Predicting species distribution: offering more than simple habitat models. Ecology Letters 8:993–1009.

Hagerman, F. B. 1952. The biology of the Dover sole, Microstomus pacificus (Lockington). Fish Bulletin 85:39.

Hicks, A. C., and C. Wetzel. 2011. The status of Dover sole (Microstomus pacificus) along the

This article is protected by copyright. All rights reserved

Author Manuscript

U.S. West Coast in 2011. National Marine Fisheries Service, Northwest Fisheries Science Center, Seattle, Washington, USA.

Hoeting, J. A. 2009. The importance of accounting for spatial and temporal correlation in analyses of ecological data. Ecological Applications 19:574–577.

Holand, A. M., I. Steinsland, S. Martino, and H. Jensen. 2013. Animal models and integrated nested Laplace approximations. G3 3:1241–1251.

Holland, D. S., and J. G. Sutinen. 2000. Location choice in New England trawl fisheries: old habits die hard. Land Economics 76:133.

Jacobson, L., J. Brodziak, and J. Rogers. 2001. Depth distributions and time-varying bottom trawl selectivities for Dover sole (Microstomus pacificus), sablefish (Anoplopoma fimbria), and thornyheads (Sebastolobus alascanus and S. altivelis) in a commercial fishery. Fishery Bulletin 99:309–327.

Kareiva, P., A. Chang, and M. Marvier. 2008. Development and conservation goals in World Bank projects. Science 321:1638–1639.

Keller, A. A., J. R. Wallace, B. H. Horness, O. S. Hamel, and I. J. Stewart. 2012. Variations in eastern North Pacific demersal fish biomass based on the U.S. west coast groundfish bottom trawl survey (2003–2010). Fishery Bulletin 110:205–222.

Krnjajić, M., A. Kottas, and D. Draper. 2008. Parametric and nonparametric Bayesian model specification: a case study involving models for count data. Computational Statistics and Data Analysis 52:2110–2128.

Krigsman, L. M., M. M. Yoklavich, E. J. Dick, and G. R. Cochrane. 2012. Models and maps: predicting the distribution of corals and other benthic macro-invertebrates in shelf habitats. Ecosphere 3:art3.

Landry, M. R., J. R. Postel, W. K. Peterson, and J. Newman. 1989. Broad-scale distributional patterns of hydrographic variables on the Washington/Oregon shelf. Pages 1–40 in M. R. Landry and B. M. Hickey, editors. Coastal oceanography of Washington and Oregon. Elsevier, Amsterdam, The Netherlands.

Latimer, A. M., S. Banerjee, H. Sang, E. S. Mosher, and J. A. Silander. 2009. Hierarchical models facilitate spatial analysis of large data sets: a case study on invasive plant species in the northeastern United States. Ecology Letters 12:144–54.

Legendre, P. 1993. Spatial autocorrelation: trouble or new paradigm? Ecology 74:1659–1673.

This article is protected by copyright. All rights reserved

Author Manuscript

Liaw, A., and M. Wiener. 2002. Classification and regression by randomForest. R News 2(3):18–22.
Lindgren, F., H. Rue, and J. Lindström. 2011. An explicit link between Gaussian fields and Gaussian Markov random fields: the stochastic partial differential equation approach. Journal of the Royal Statistical Society Series B 73:423–498.
Maunder, M. N., and A. E. Punt. 2004. Standardizing catch and effort data: a review of recent approaches. Fisheries Research 70:141–159.
NMFS [National Marine Fisheries Service]. 2013. Groundfish essential fish habitat synthesis: a report to the Pacific Fishery Management Council. National Oceanic and Atmospheric Administration, Northwest Fisheries Science Center, Seattle, Washington, USA.
National Oceanic and Atmospheric Administration [NOAA]. 2001. U.S. vector shoreline derived from NOAA nautical charts. NOAA Ocean Service, Office of Coast Survey, Silver Spring, Maryland, USA.
National Oceanic and Atmospheric Administration [NOAA]. 2003. U.S. Coastal Relief Model: Northwest Pacific. National Geophysical Data Center, Boulder, Colorado, USA.
Robinson, L. M., J. Elith, A. J. Hobday, R. G. Pearson, B. E. Kendall, H. P. Possingham, and A. J. Richardson. 2011. Pushing the limits in marine species distribution modelling: lessons from the land present challenges and opportunities. Global Ecology and Biogeography 20:789–802.
Rue, H., and S. Martino. 2007. Approximate Bayesian inference for hierarchical Gaussian Markov random field models. Journal of Statistical Planning and Inference 137:3177–3192.
Rue, H., S. Martino, and N. Chopin. 2009. Approximate Bayesian inference for latent Gaussian models by using integrated nested Laplace approximations. Journal of the Royal Statistical Society Series B 71:319–392.
Saas, Y., and F. Gosselin. 2014. Comparison of regression methods for spatially-autocorrelated count data on regularly- and irregularly-spaced locations. Ecography 37:1–14
Schrödle, B., and L. Held. 2011. Spatio-temporal disease mapping using INLA. Environmetrics 22:725–734.
Shelton, A. O., J. T. Thorson, E. J. Ward, and B. E. Feist. 2014. Spatial, semi-parametric models improve estimates of species abundance and distribution. Canadian Journal of Fisheries and Aquatic Sciences 71:1655–1666.
Spiegelhalter, D. J., N. G. Best, B. P. Carlin, and A. van der Linde. 2002. Bayesian measures of

This article is protected by copyright. All rights reserved

Author Manuscript

model complexity and fit. Journal of the Royal Statistical Society Series B 64:583–639.
Sundblad, G., U. Bergström, and A. Sandström. 2011. Ecological coherence of marine protected area networks: a spatial assessment using species distribution models. Journal of Applied Ecology 48:112–120.
Thorson, J. T., A. O. Shelton, E. J. Ward, and H. J. Skaug. 2015. Geostatistical delta-generalized linear mixed models improve precision for estimated abundance indices for West Coast groundfishes. ICES Journal of Marine Science 72(9):2674–2683.
Thorson, J. T., and E. Ward. 2013. Accounting for space-time interactions in index standardization models. Fisheries Research 147:426–433.
Toole, C., R. Brodeur, C. Donohoe, and D. Markle. 2011. Seasonal and interannual variability in the community structure of small demersal fishes off the central Oregon coast. Marine Ecology Progress Series 428:201–217.
van Putten, I. E., S. Kulmala, O. Thébaud, N. Dowling, K. G. Hamon, T. Hutton, and S. Pascoe. 2012. Theories and behavioural drivers underlying fleet dynamics models. Fish and Fisheries 13:216–235.
Ward, E. J., J. E. Jannot, Y. Lee, K. Ono, A. O. Shelton, and J. T. Thorson. 2015. Using spatiotemporal species distribution models to identify temporally evolving hotspots of species co-occurrence. Ecological Applications 25(8):2198–2209.
Ward, T., and M. Vanderklift. 1999. Selecting marine reserves using habitats and species assemblages as surrogates for biological diversity. Ecological Applications 9:691–698.
Whittaker, R., S. Levin, and R. Root. 1973. Niche, habitat, and ecotope. American Naturalist 107:321–338.
Worm, B., et al. 2009. Rebuilding global fisheries. Science 325:578–85.
Zuur, A. F., E. N. Ieno, N. J. Walker, A. A. Saveliev, and G. M. Smith. 2009. Mixed effects models and extensions in ecology with R. Springer, New York, New York, USA.

SUPPLEMENTAL MATERIAL

Ecological Archives

Appendices A–C and the Supplement are available online: http://dx.doi.org/10.1890/14-1874.1.sm

Table 1. Parameter definition and prior specifications in INLA.

Parameter	Symbol	Prior (non-informative)

This article is protected by copyright. All rights reserved

Author Manuscript

Fixed effects	β	N(0, 1000)
Precision for the measurement error	$1/\sigma_p^2$	Gamma(1;5e–05)
Spatial precision	τ_p^2	Gamma(1;5e–05)
Spatial range	$2/\kappa$	Gamma(1;5e–05)

Table 2. Covariates selection results for the spatio-temporal generalized linear models (GLMs).

Model	Variables	Delta DIC	Mean(LS)	P value
1+	D+D2+T+T2+S+S2+R	0.00	1.683	ref
	D+D2+T+T2+S+R	3.83	1.683	0.986
	D+D2+T+T2+S	0.69	1.683	0.998
	D+D2+T+T2+R	3.14	1.683	0.982
	D+D2+T+S+S2+R	8.97	1.693	0.784
	D+D2+T+S+S2	4.86	1.693	0.795
	D+D2+T+S+R	12.70	1.694	0.761
	D+D2+T+R	9.96	1.694	0.767
	D+D2+T+S	9.59	1.693	0.776
	D+D2+T	9.54	1.694	0.778
	D+D2+T+T2	3.06	1.683	0.987
	D+D2+R+S+S2	25.10	1.696	0.722
	D+D2+R+S	29.26	1.696	0.709
	D+D2+R	26.36	1.696	0.727
	D+D2+S+S2	23.08	1.696	0.730
	D+D2+S	28.19	1.696	0.728
	D+D2	28.72	1.696	0.731
2+	D+D2+T+T2+S+S2+R	23.69	1.695	0.952
	D+D2+T+T2+S+R	26.99	1.694	0.968
	D+D2+T+T2+S	24.72	1.692	ref
	D+D2+T+T2+R	24.66	1.694	0.975
	D+D2+T+S+S2+R	82.87	1.711	0.619
	D+D2+T+S+S2	86.91	1.712	0.610
	D+D2+T+S+R	92.49	1.713	0.578

This article is protected by copyright. All rights reserved

Author Manuscript

	D+D2+T+R	91.54	1.713	0.586
	D+D2+T+S	98.16	1.714	0.581
	D+D2+T	96.40	1.713	0.876
	D+D2+T+T2	38.14	1.695	0.951
	D+D2+R+S+S2	0.00	1.697	0.908
	D+D2+R+S	7.45	1.698	0.891
	D+D2+R	7.85	1.697	0.905
	D+D2+S+S2	4.62	1.697	0.899
	D+D2+S	13.23	1.698	0.870
	D+D2	11.36	1.698	0.892
1−	D+D2+T+T2+S+S2+R	8.25	0.279	0.915
	D+D2+T+T2+S+R	16.24	0.280	0.869
	D+D2+T+T2+S	24.60	0.282	0.828
	D+D2+T+T2+R	13.90	0.280	0.885
	D+D2+T+S+S2+R	8.58	0.278	0.931
	D+D2+T+S+S2	16.16	0.280	0.879
	D+D2+T+S+R	13.92	0.279	0.896
	D+D2+T+R	11.53	0.279	0.916
	D+D2+T+S	22.16	0.281	0.844
	D+D2+T	22.65	0.281	0.843
	D+D2+T+T2	24.58	0.282	0.820
	D+D2+R+S+S2	0.00	0.276	ref
	D+D2+R+S	5.00	0.277	0.974
	D+D2+R	1.39	0.276	0.998
	D+D2+S+S2	9.96	0.278	0.937
	D+D2+S	15.67	0.279	0.901
	D+D2	16.33	0.279	0.898
2−	D+D2+T+T2+S+S2+R	0.00	0.277	ref
	D+D2+T+T2+S+R	3.46	0.278	0.986
	D+D2+T+T2+S	4.09	0.278	0.983
	D+D2+T+T2+R	3.32	0.278	0.989

Author Manuscript

This article is protected by copyright. All rights reserved

D+D2+T+S+S2+R	13.18	0.280	0.917
D+D2+T+S+S2	13.48	0.280	0.907
D+D2+T+S+R	16.84	0.280	0.900
D+D2+T+R	16.21	0.280	0.902
D+D2+T+S	16.83	0.280	0.896
D+D2+T	16.35	0.280	0.908
D+D2+T+T2	3.45	0.278	0.987
D+D2+R+S+S2	16.78	0.280	0.910
D+D2+R+S	19.8	0.281	0.888
D+D2+R	17.29	0.280	0.902
D+D2+S+S2	16.86	0.280	0.899
D+D2+S	19.49	0.281	0.891
D+D2	17.41	0.279	0.905

Notes: Model selection was performed for the Dover sole presence/absence at survey pass 1 (1−) and survey pass 2 (2−); and for Dover sole density at each survey pass (1+ and 2+). Deviance information criterion (DIC) and the mean logarithmic score are used jointly to determine the best model (highlighted in bold). In case of conflicting result between DIC and the mean logarithmic score, the best model was chosen based on DIC as the difference in mean logscore was rarely significantly different (the P values). Abbreviations are D (log of depth), T (temperature), S (sediment size), and R (distance to closest rocks). D2 and T2 are for squared covariate effect

FIG. 1. Map of the U.S. west coast along with the survey sites from 2004 to 2011.

FIG. 2. Panels (a–h) are biomass maps of Dover sole along the U.S. west coast between 2004 and 2011. For each year, the posterior mean estimate of biomass at the first survey pass (1) and at the second survey pass (2) are put side by side.

FIG. 3. Marginal posterior effects of haul depth, distance to rock, and sediment size on the Dover sole biomass for pass 1 and pass2. To show the marginal effects, all covariates not of interest are held at the mean. The relationship is shown across the entire observed scale, and the rug plot (i.e., ticks at the bottom of each plot) indicates the distribution of data; t is year.

FIG. 4. Panels (a–i) show the difference in average biomass between the second survey pass and the first survey pass plotted against catch for each fished grid along the U.S. west coast and year.

This article is protected by copyright. All rights reserved

Author Manuscript

The darker the shading or the lines, the more data points are concentrated in the area. The lines corresponds to the kernel density estimates

FIG. 5. Panels (a–h) show 2004–2011 median estimate of net change in biomass between pass 1 and pass 2 within the same year (NCB_1), and between pass 2 of year t i and pass 1 of year t + 1 (NCB_2), for each 2 × 2 km spatial grid along the U.S. west coast.

FIG. 6. Panel (a) shows annual survey locations between 2004 and 2011. Panel (b) shows the median across the 2004–2011 median estimate of net change in biomass between pass 1 and pass 2 within the same year (NCB_1), for each 2 × 2 km spatial grid along the U.S. west coast. Panel (c) shows the median across the 2004–2010 median estimate of net change in biomass between pass 2 of year t and pass 1 of year t + 1 (NCB_2), for each 2 × 2 km spatial grid along the U.S. west coast. Panels (d) is a plot of median NCB_1 vs. median NCB_2.

FIG. 7. Panel (a) shows depth distribution along the west coast, (b) is distance to nearest rock outcrops along the west coast, (c) is variable importance plot for the predictor variables from the random forest (RF) used for predicting the net change in biomass (NCB_1) between pass 2 and pass 1 within the same year. Panels (d–g) are partial dependence plots for RF for NCB_1 and four predictor variables. Partial dependence is the dependence of NCB_1 on one predictor variable after averaging out the effects of the other predictor variables in the model. RF is run on 100 Monte Carlo samples of NCB_1 by year to account for the distribution uncertainty in NCB_1. Results for each year are color coded in gray intensity.

FIG. 8. Panel (a) shows depth distribution along the west coast, (b) is distance to nearest rock outcrops along the west coast, (c) is variable importance plot for the predictor variables from the random forest (RF) used for predicting the net change in biomass between pass 1 and pass 2 of different years (NCB_2). Panels (d–g) are partial dependence plots for RF for NCB_2 and four predictor variables. RF is run on 100 Monte Carlo samples of NCB_2 by year to account for the distribution uncertainty in NCB_2. Results for each year are color coded in gray intensity.

Author Manuscript

This article is protected by copyright. All rights reserved

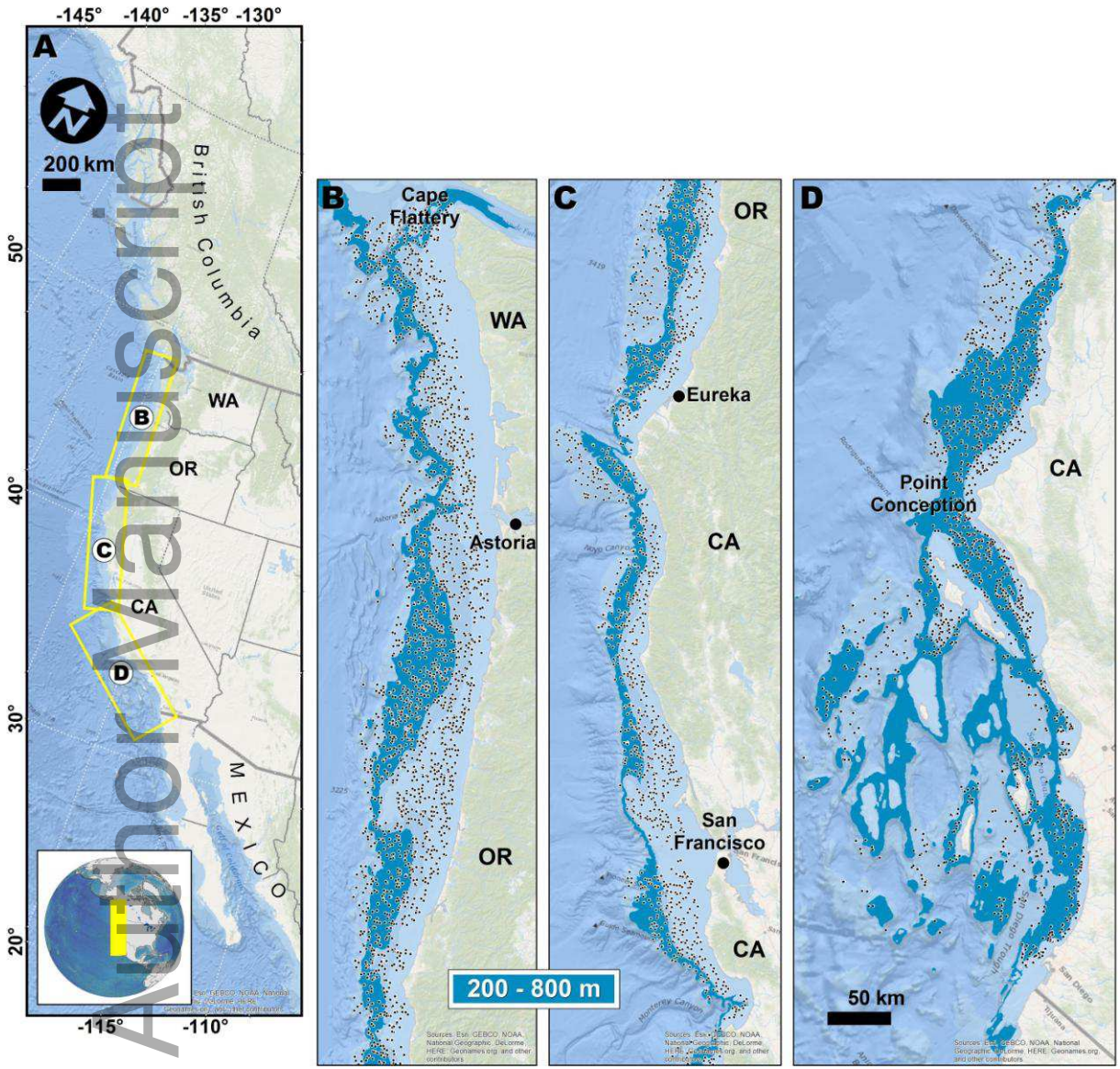

1

2 Figure 1

This article is protected by copyright. All rights reserved

Author Manuscript

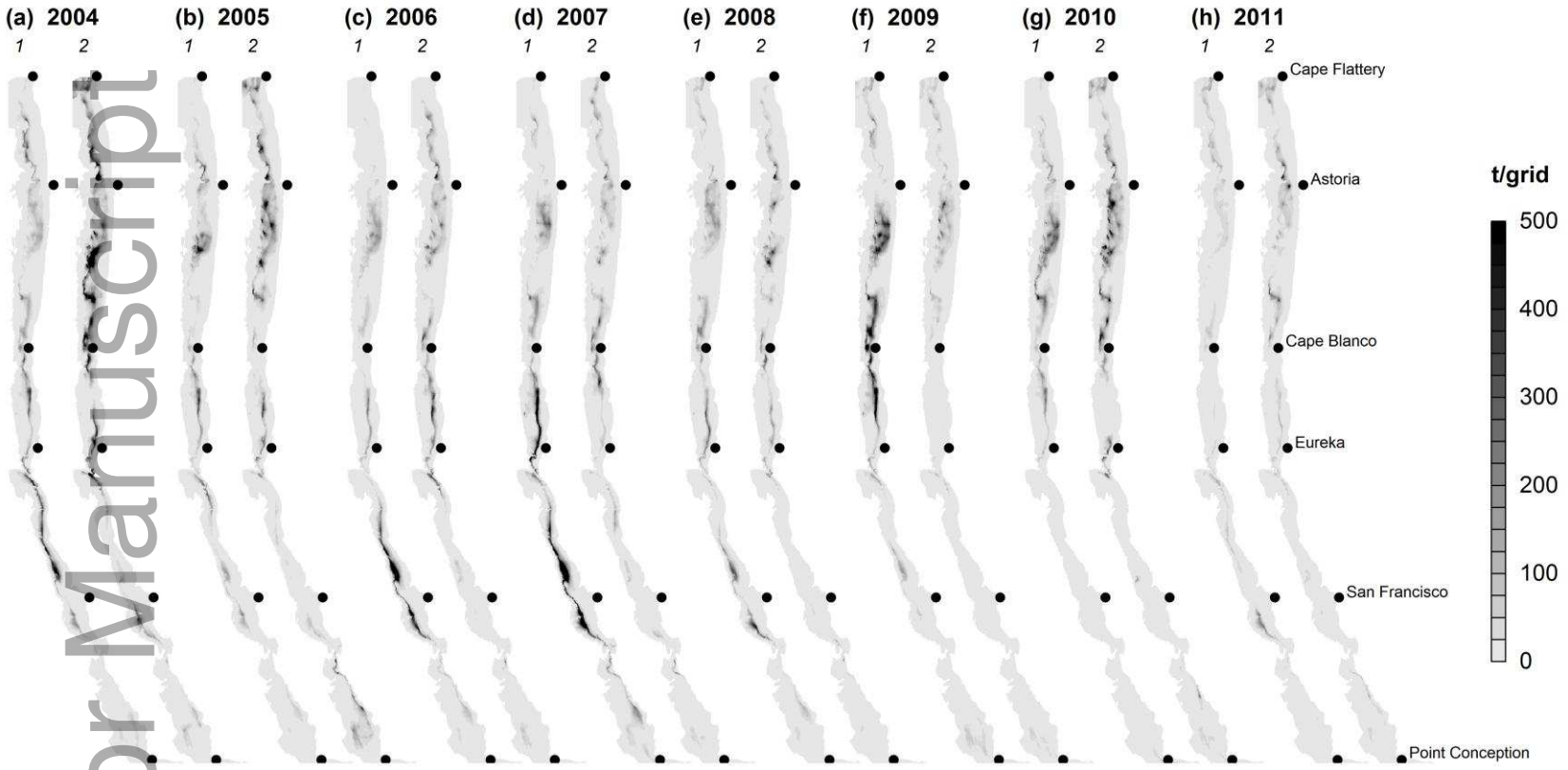

Figure 2:

This article is protected by copyright. All rights reserved

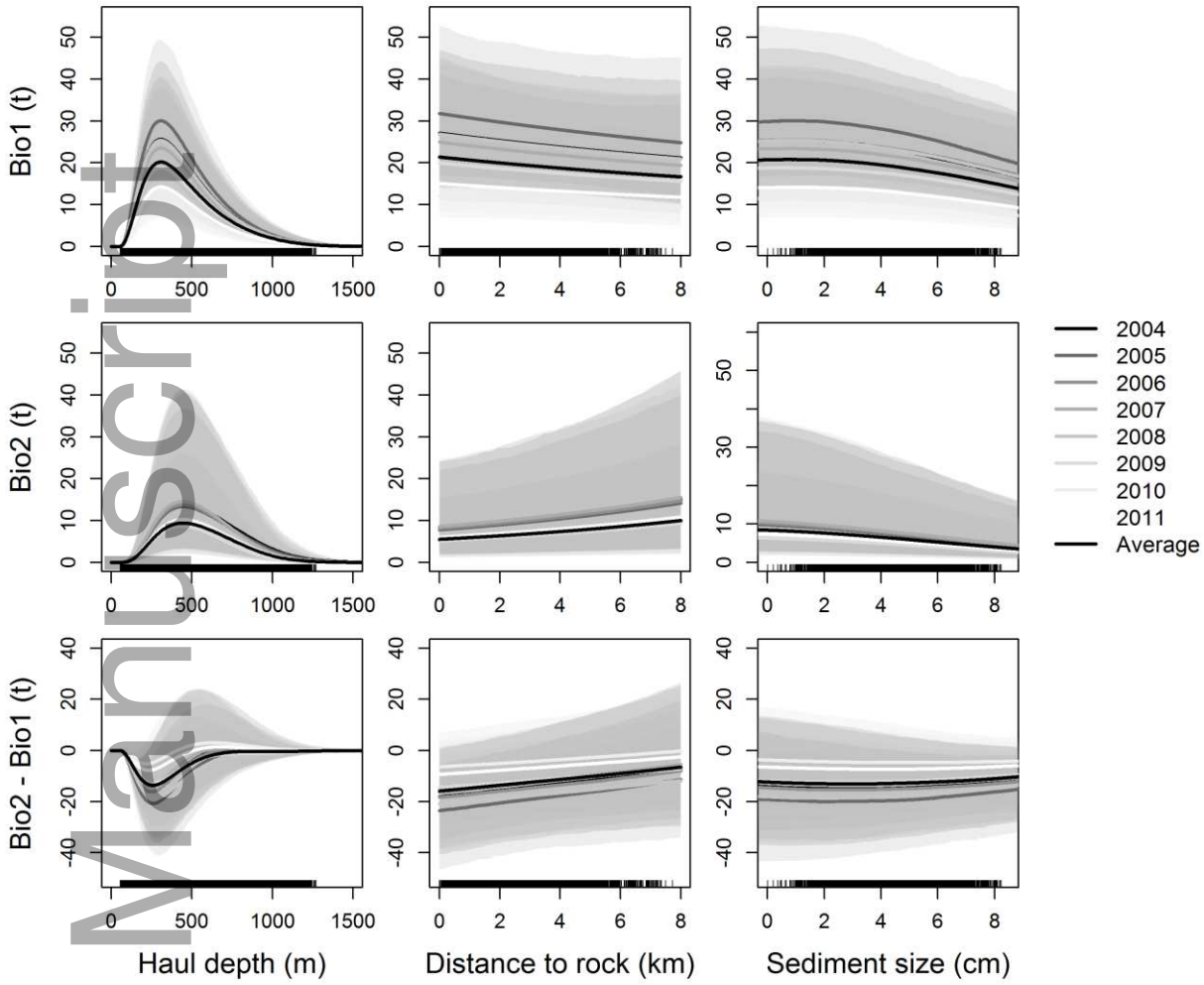

Figure 3:

Author Manuscript

This article is protected by copyright. All rights reserved

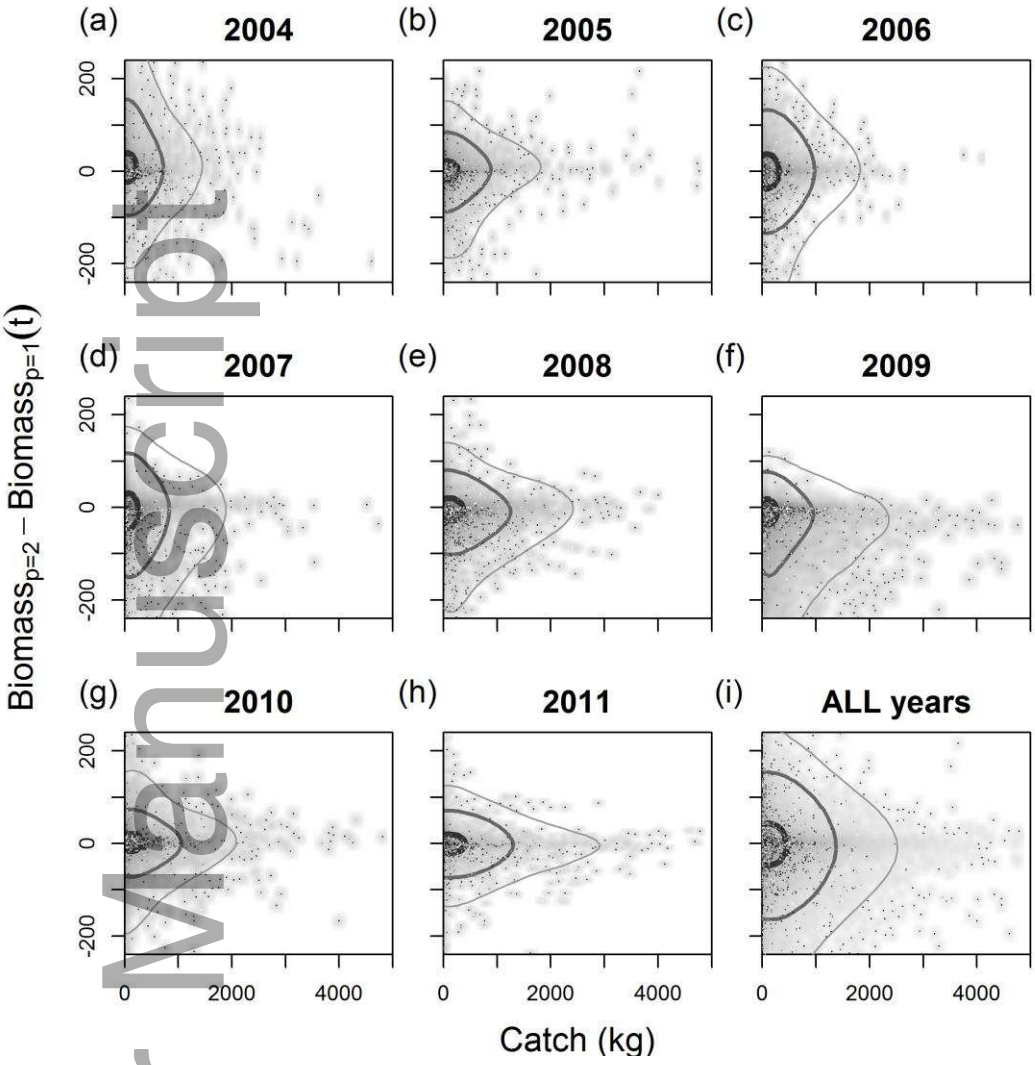

Figure 4:

Author Manuscript

This article is protected by copyright. All rights reserved

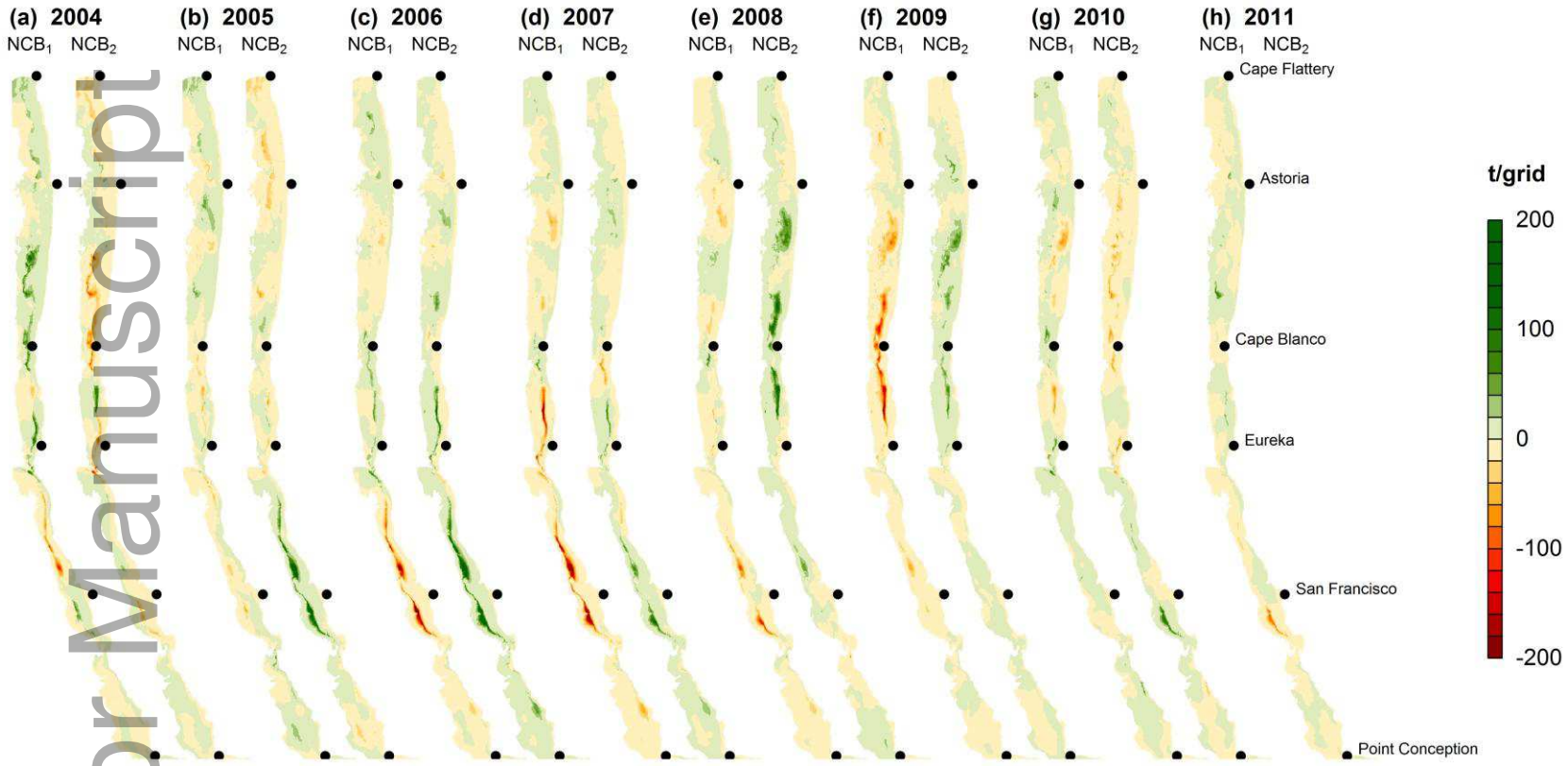

Figure 5

Author Manuscript

This article is protected by copyright. All rights reserved

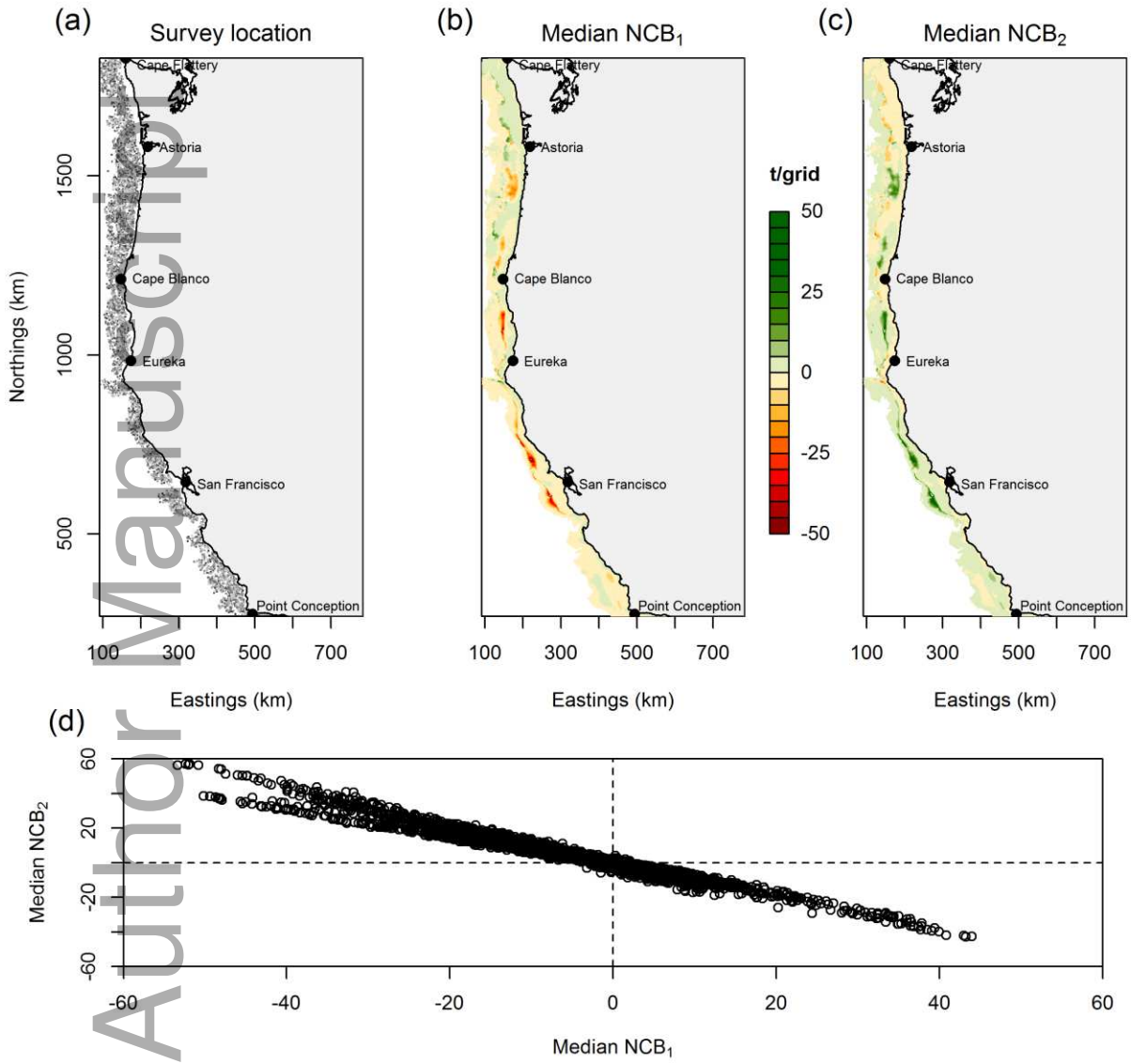

Figure 6

This article is protected by copyright. All rights reserved

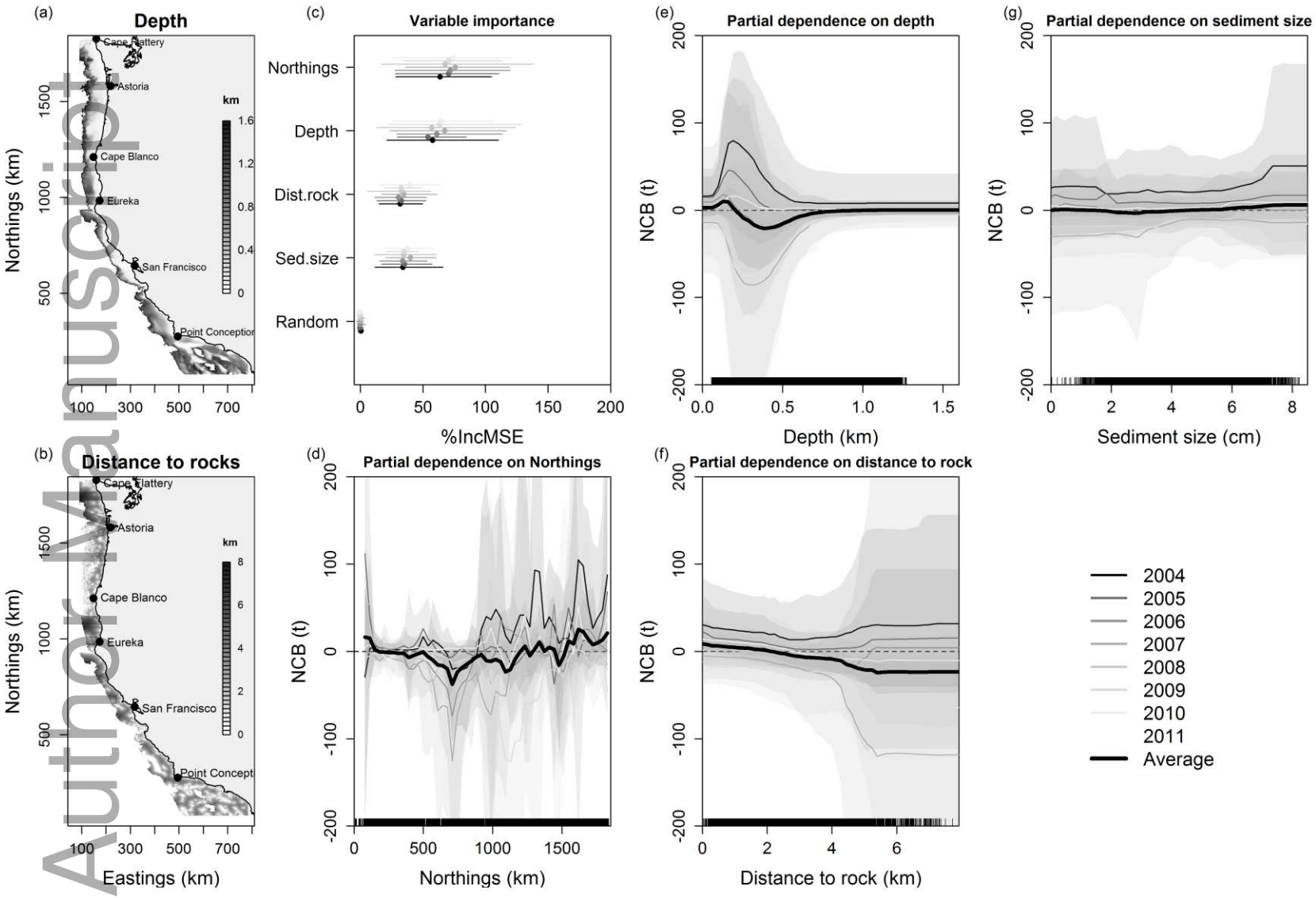

Figure 7

This article is protected by copyright. All rights reserved

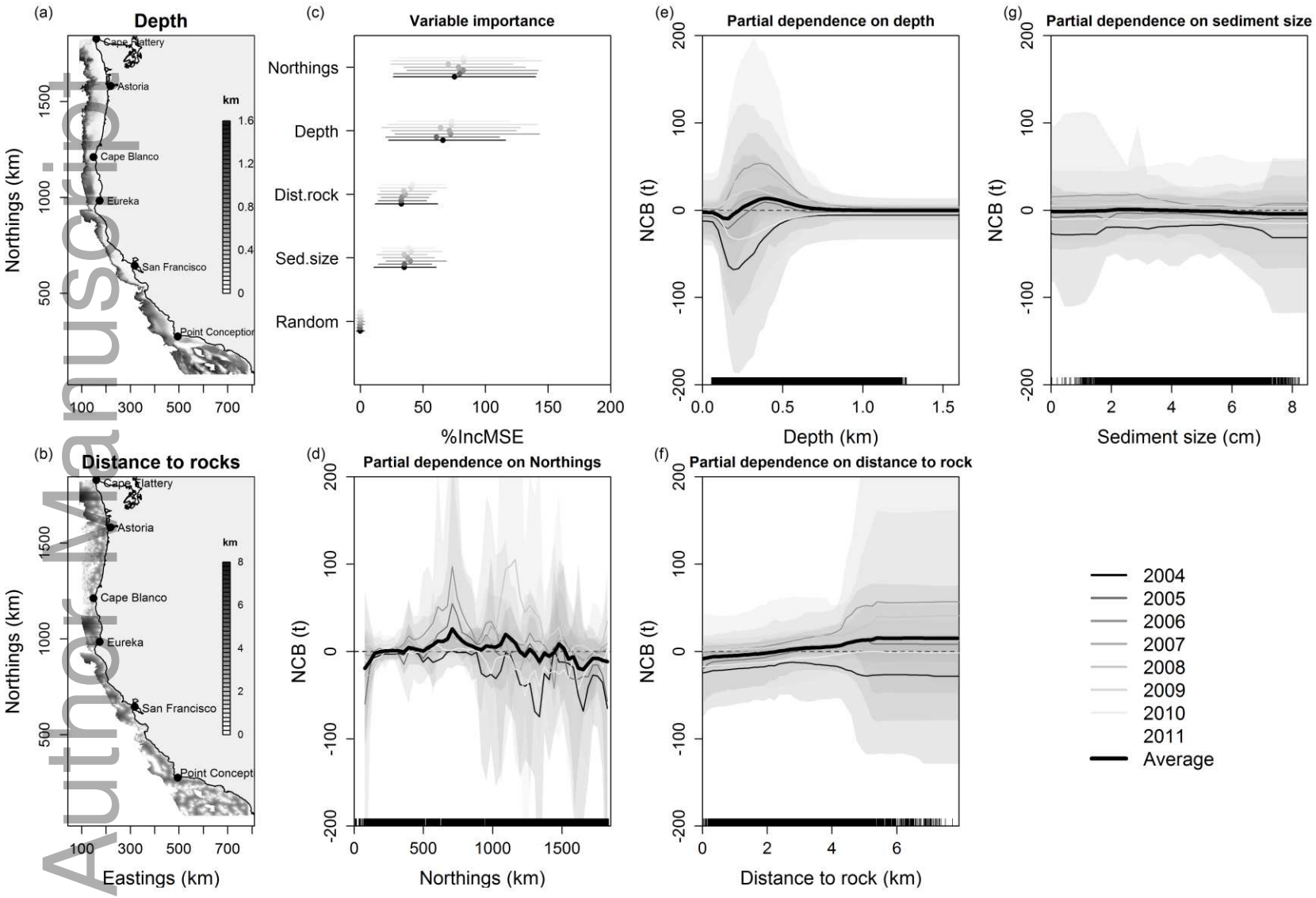

Figure 8

This article is protected by copyright. All rights reserved